

Safety Assessment of a Liquid Rocket in Launching Site Under Earthquake Wave EI

Jinghui Li¹, Xueren Wang¹, Jiazhao Chen^{1,*}, Xuan Zhang², Jiexin Weng² and Gang Bai²

¹PLA Rocket Force University of Engineering, Xi'an, China

²Inner Mongolia Power Machinery Research Institute, Hohhot, China

*Corresponding author

Abstract: By adopting time history method in software ANSYS, dynamic response of a liquid rocket was analyzed when it is suffered from earthquake wave EI in a launching site, and the displacement and stress of the rocket was calculated before and after it was fueled, and the safety of the liquid rocket was evaluated. The result showed that the liquid rocket swung along the acting direction of the earthquake wave both before and after it was fueled under earthquake wave EI. The higher the position of the rocket, the larger the swing. And the maximum displacement located on the top of the rocket, and the maximum stress located at the support places on the rear part. The maximum swing and maximum stress, after it was fueled, increased a lot from those before it was fueled, so the rocket has the possibility to fall down and to damage in structure.

Keywords: Earthquake wave EI; liquid rocket; dynamic response; launching site; safety assessment.

1. Introduction

Before launching a large liquid carrier rocket, it is usually vertically erected on the launch pad for a series of tests and propellant refueling. Is there a risk of liquid rocket overturning under the action of seismic waves if an earthquake occurs at this time? This is a major issue related to the safety of the shooting range, and it is necessary to conduct in-depth research.

Domestic and foreign scholars have conducted in-depth and persistent research on the seismic resistance of buildings and storage tanks[1][2]. Since the 1930s, a series of calculation theories, experimental techniques, and design specifications have been proposed for the seismic research of vertical liquid storage tanks[3][4]. With the development of finite element technology, numerical simulation methods are widely used for seismic response analysis of storage tanks, fully considering the influence of various nonlinear factors and liquid-solid coupling, analyzing the inherent characteristics and dynamic response of storage tanks, and calculating the lifting and buckling effects of storage tanks under seismic action. Domestic and foreign scholars have also conducted in-depth research on the dynamic characteristics of launch vehicles, including rocket structural dynamics modeling theory and modeling technique[5][6], Dynamic testing technology, dynamic model correction technology, effective load coupling response analysis and vibration control technology, dynamic analysis of liquid-solid coupling vibration between propellant and storage tank, etc[7][8], this has laid a solid foundation for the design of rocket payload environment, attitude stability control system, and the stability design of self-excited vibration (POGO) generated by the coupling of structural vibration and propulsion system. However, there are relatively few research reports on the dynamic characteristics and response of liquid rockets under seismic waves. Liu Caizhi and Tang Guojin studied the seismic response and seismic design of a certain type of carrier rocket in an upright state[9], the main body of the rocket adopts a beam element model, and only a fine 3D model is used locally. The vertical state of liquid rockets is

similar to that of vertical storage tanks, and the seismic research results of vertical storage tanks can serve as an important reference for the seismic response analysis of liquid rockets. This article uses the finite element analysis software ANSYS to establish a three-dimensional fine model of a liquid rocket, taking typical EI seismic waves as input, considering the influence of liquid-solid coupling, and using the time history method to calculate the dynamic response of the liquid rocket before and after propellant filling. The movement trend and stress changes of the rocket under seismic action are obtained, and the possibility of danger of the liquid rocket under EI wave action is evaluated, providing reference for the safe use of the target range.

2. Computation Model

2.1. Geometric model

This article takes a two-stage liquid launch vehicle as an example, which mainly consists of a fairing (containing payload), an instrument compartment, a secondary power system (including a secondary oxidizer storage tank, a secondary tank compartment, and a secondary combustion agent storage tank), an interstage section (including an interstage shell section and an interstage rod section), and a primary power system (including a primary oxidizer storage tank, a primary tank compartment, and a primary combustion agent storage tank). To reduce the computational scale, the modeling ignored the fairing (containing payload) and instrument compartment, and only established the main body of the rocket. However, in the calculation, the fairing (containing payload) and instrument compartment were loaded as mass forces onto the short shell in front of the secondary oxidizer storage tank. When the rocket stands upright on the launch pad, it is supported by four parts on the short shell behind the primary combustion chamber. The geometric model of the liquid rocket is shown in Figure 1 (a).

When modeling, the shell is treated as a light shell and the middle surface is extracted, which reduces the number of elements and improves computational efficiency while ensuring the authenticity of the model. Establish a propellant

model[10] using the fill command to fill the surfaces of each tank, then cut to obtain liquid propellant models under different liquid filling states, and finally remove unnecessary

liquid propellant parts from the tank through suppression operations. This article sets the propellant filling volume ratio after filling to 80%, as shown in Figure 1 (b).

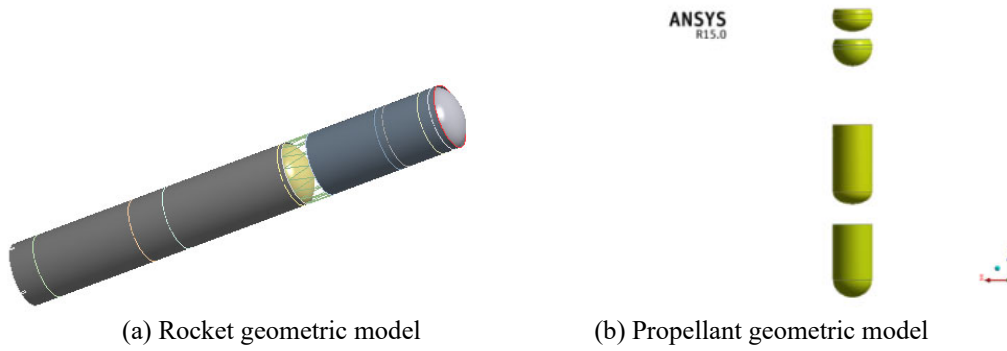


Figure 1. Geometric Model of Structure

2.2. Finite element model

This article uses the SHELL181 shell element to mesh the shell structure, and the connecting rods between stages are divided using the beam element BEAM188. In the process of grid partitioning, in order to obtain high-quality units, the unit size was controlled to 0.05m, resulting in a total of 149406 nodes and 148037 units.

The liquid filling part is divided into FLUID30 units. In order to make the structure fluid element mesh share nodes, the outer surfaces of the fluid structures in four propellant storage tanks were selected, and the control size was also set to 0.05m. Finally, the finite element model of the liquid rocket was obtained under 80% liquid filled conditions. After

refueling, a total of 1038233 nodes and 666136 units were obtained, including 888827 nodes and 518099 units for the liquid part.

3. Calculation Settings

3.1. Material properties

The first and second stage shell materials of the rocket are made of aluminum alloy, the interstage rods are made of alloy steel, the oxidizer is nitrogen tetroxide, and the combustion agent is unsymmetrical dimethylhydrazine. The material properties are shown in Table 1 and defined in the ANSYS material library.

Table 1. Material Property of Liquid Rocket

Material	Parameter	Numerical value
Aluminum alloy	Elastic modulus (E/MPa)	7×10^4
	Yield limit (σ_s/MPa)	400
	Poisson's ratio (μ)	0.33
	Density ($\rho/\text{kg/m}^3$)	2270
Alloy steel	Elastic modulus (E/MPa)	2×10^5
	Yield limit (σ_s/MPa)	450
	Poisson's ratio (μ)	0.3
	Density ($\rho/\text{kg/m}^3$)	7850
Nitrogen tetroxide	Liquid density ($\rho/\text{kg/m}^3$)	1446
	Sound velocity in liquid ($v/\text{m/s}$)	1013
UDMH	Liquid density ($\rho/\text{kg/m}^3$)	793
	Sound velocity in liquid ($v/\text{m/s}$)	1444

3.2. Constraints and load conditions

Before launching, the rocket is supported on the launch pad by a short shell behind the first stage combustion agent storage tank. This area is treated as a fixed support. In the finite element model of a liquid rocket, four symmetrically centered rectangular areas on the tail of the first stage are taken for marking calibration, limiting the movement of all elements in the x, y, and z directions and their rotation around each axis in the marking area.

Then apply the load. The liquid rocket is unloaded before refueling, and after refueling, the liquid volume ratio in each tank is 80%. The rocket is only subjected to its own gravity, the static water pressure of the internal propellant, and the front and rear mass loads in an upright state, so four types of loads are applied here:

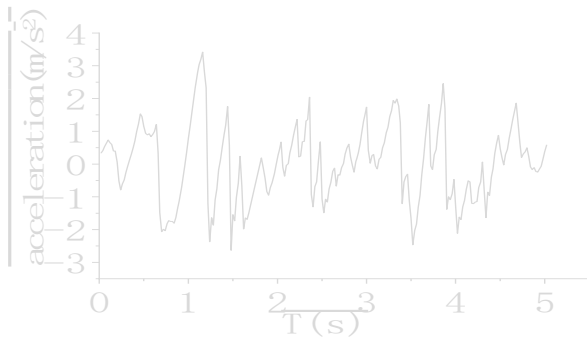
(1) Gravitational acceleration. Select all units and apply the gravitational acceleration in the z-direction under the inertial load (Acceleration of Gravity) $g=9.8\text{m/s}^2$.

(2) Hydrostatic pressure. Apply static water pressure on the

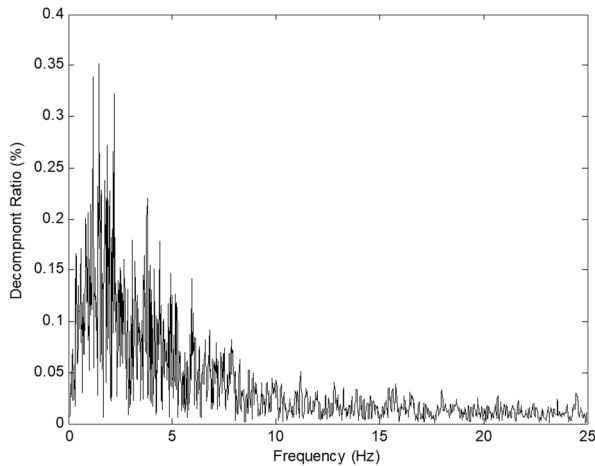
surfaces of the four storage tanks, Define the propellant density in each level of combustion agent storage tank and oxidizer storage tank separately, and define the liquid level height in each tank to ensure that the filling volume meets the volume ratio 80%.

(3) Mass load. In the z-direction, define the mass load on the front frame of the secondary oxidizer tank so that its resultant force is equal to the equivalent mass force of the fairing (as well as the payload and instrument compartment).

(4) Earthquake waves. In this article, the time history method is used for seismic response analysis, and the time-domain acceleration input method is used for seismic wave loading. This article selects the EI wave with relatively complete records, which belongs to the category of strong earthquake waves with a magnitude of 8. It is also the first time that humans have obtained a strong earthquake record with a maximum acceleration exceeding 0.3g. This article extracts a 5-second acceleration sequence, including the maximum acceleration peak, and loads it from the X direction of the support part. The time history curve and frequency spectrum of seismic waves are shown in Figure 2.



(a) 5S acceleration time history curve of EI wave



(b) EI wave frequency distribution

Figure 2. Earthquake Wave EI

3.3. Fluid structure coupling setting

In calculations, the flow field elements and structural elements need to be coupled with degrees of freedom at the contact surface. At the same time, the contact surface between the liquid propellant and air in each storage tank belongs to the free liquid surface, so control command flow must be

applied to these two surfaces.

(1) Define the fluid structure coupling surface, select the nodes on the contact surface between the structural unit and the fluid unit, and then select the sound field units associated with these nodes. Apply the fsi command to achieve degree of freedom coupling on the contact surface between the structural and fluid units;

(2) To define a free liquid surface, first define the contact surface between propellant and air in each tank as face1. Apply the free command on face1. As the tank is filled with protective gas at three atmospheres, a pressure of 0.3 MPa needs to be defined above the free liquid surface. Finally, add gravity to the model, select all units, and define the gravitational acceleration as 9.8m/s^2 .

3.4. Calculation step size setting

The seismic response analysis in this article adopts the time history method, and the Newmark time integration method is used in ANSYS to solve the control equation at discrete time points. The initial step size is determined by the following formula:

$$\Delta t_{initial} = \frac{1}{25 f_{response}} \quad (1)$$

Among them, $f_{response}$ Indicates the frequency of the highest mode of vibration that is of concern when studying the structure.

Modal analysis was conducted on the structures before and after refueling, and the highest frequencies of the first and second modes were found to be 4.05023Hz and 1.6342Hz, respectively. According to formula (1), the initial time steps before and after refueling were 0.01s and 0.025s, respectively.

4. Analysis of Calculation Results

This article calculates the dynamic response of the structure under the action of EI seismic waves in two states before and after injection. The seismic wave loading time is 5 seconds, and the stress and displacement of the structure within the 5 second time are obtained.

4.1. The motion trend of the rocket before refueling under the action of EI waves

The displacement data of the liquid rocket under the action of EI wave before filling are calculated. The analysis shows that the whole liquid rocket swings roughly along the x-axis direction, the swing amplitude increases from small to large within 5S, and finally tends to be stable. The maximum swing amplitude is about 0.095m, and the swing period is about 0.4s.

In order to analyze the displacement change of the overall structure of the liquid rocket under the time history, the total displacement of the initial, trough, peak and end time in one cycle after its stable swing is studied, as shown in Figure 3. Corresponding to the total displacement nephogram at 4.156s, 4.26s, 4.476s and 4.59s. For the convenience of observing the movement trend, the overall variation amplitude of the two peak periods of 4.26s and 4.476s was amplified by 32 times.

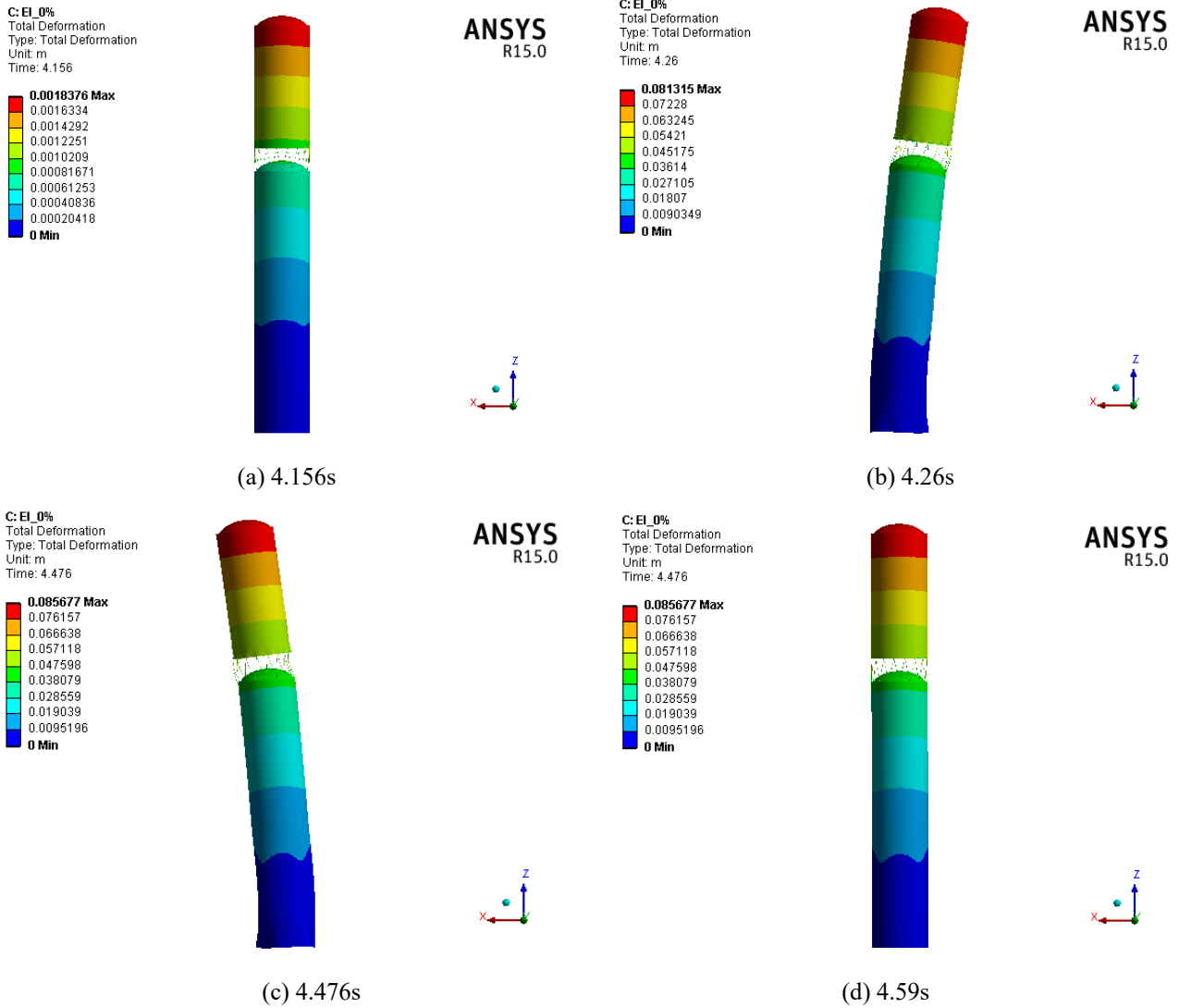


Figure 3. Total Displacement Nephogram of Rocket Under Earthquake Wave EI Before Fueling

It can be seen from Figure 3 (a) that at 4.156s, the maximum displacement of the liquid rocket appears at the top of the liquid rocket, and the size is only 0.0018m, so the overall structure is basically vertical, that is, perpendicular to the XY plane; It can be seen from Figure 3 (b) that at 4.26s, the top of the liquid rocket is at the minimum displacement, and its size is about 0.0813m, swinging in the negative direction to the X axis; It can be seen from Figure 3 (c) that at 4.476s, the top of the liquid rocket is at the maximum displacement, and its size is about 0.0857m, swinging forward to the X axis; At 4.59s, the overall structure of the liquid rocket returned to the vertical state again, perpendicular to the XY plane. Therefore, in a swing period, the total displacement of the liquid rocket before filling under the action of EI wave increases with the increase of height. The maximum value appears at the top and the minimum value at the bottom. Combined with the characteristics of the period, it can be seen that the same is true in the whole time history.

From the maximum displacement, it can be seen that the liquid rocket has a large swing under the action of EI wave

before filling, but it will not endanger the stability, and the liquid rocket will not topple.

4.2. Stress of rocket under EI wave before filling

From the previous section, it can be seen that the liquid rocket oscillates periodically along the x-axis under the action of EI waves before refueling. The equivalent stress cloud maps of the initial, trough, peak, and end moments during a stable oscillation cycle are shown in Figure 4, corresponding to 4.156s, 4.26s, 4.476s, and 4.59s, respectively. For the convenience of observation, the overall change amplitude at the peak moments of 4.26s and 4.476s was also amplified by 32 times.

As shown in Figure 4, at all four moments, the maximum stress of the liquid rocket before refueling occurred near the fixed support. According to Figures 4 (b) and 4 (c), it can be seen that the maximum stress value when the liquid rocket swings to the maximum displacement is about 169MPa.

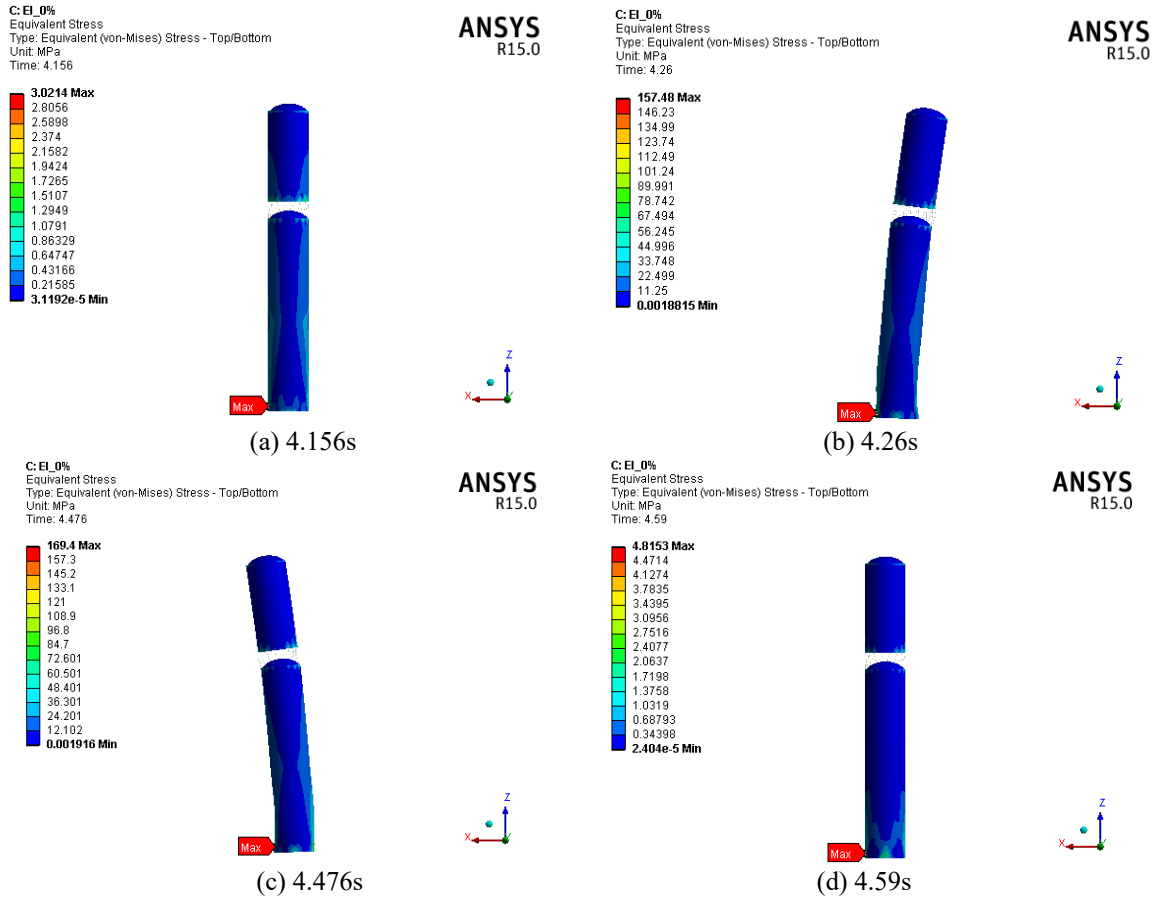


Figure 4. Equivalent Stress Nephogram of Rocket Under Earthquake Wave EI Before Fueling

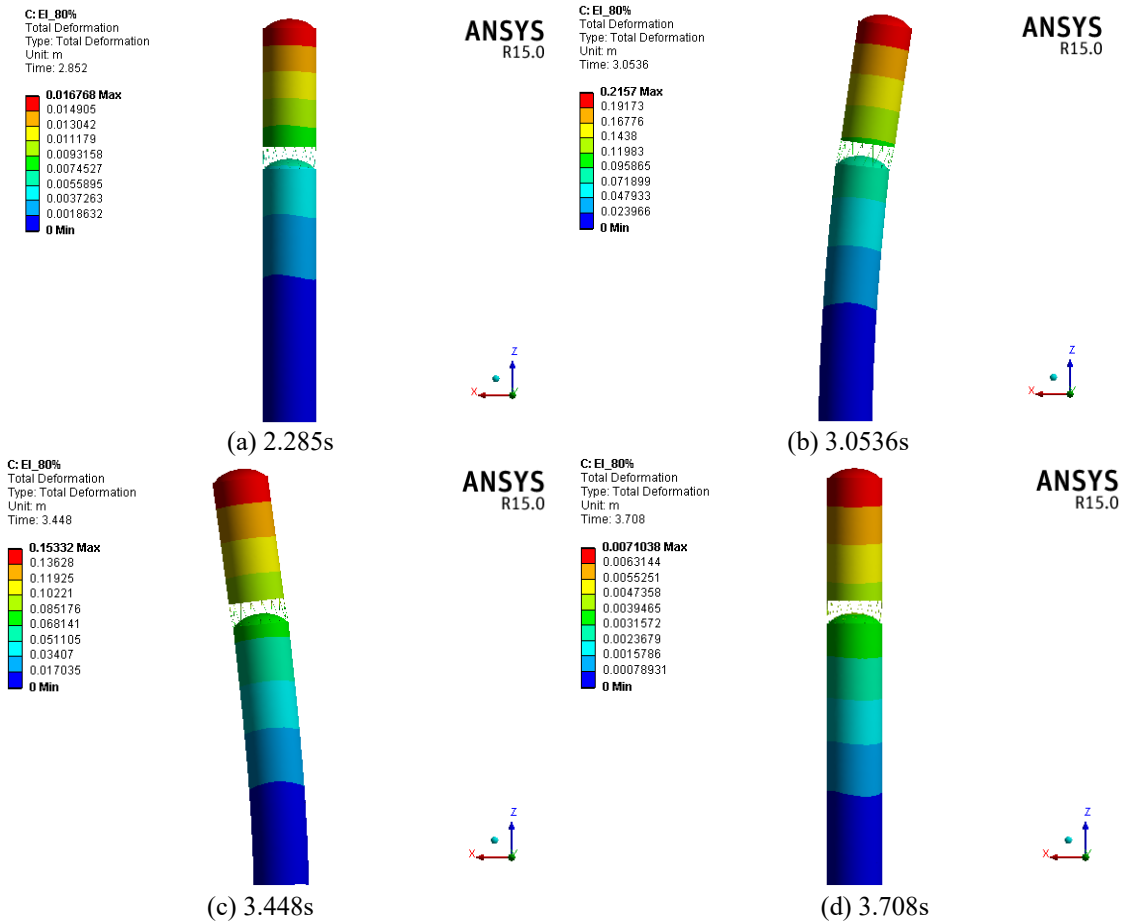


Figure 5. Total Displacement Nephogram of Rocket Under Earthquake Wave EI After Fueling

Through the analysis of all stress data, the maximum equivalent stress value in the entire time history is about 185MPa. When the safety factor is set to 1.5, the structural strength reserve coefficient is 1.4, which will not cause strength failure, but there is a possibility of instability failure.

4.3. Movement trend of rocket after filling under EI wave

According to displacement data analysis, under the action of EI waves, the overall vibration form of the liquid rocket after refueling also oscillates horizontally along the xz plane. Within 5 seconds, the oscillation amplitude increases from small to large but is not stable, with a maximum oscillation amplitude of about 0.26m and a oscillation period of about 0.9s. In order to analyze the displacement changes of the overall structure of the liquid rocket after refueling, the total displacement cloud maps of the initial, trough, peak, and end moments during one swing cycle are provided, as shown in Figure 5, corresponding to the total displacement cloud maps of 2.852s, 3.0536s, 3.448s, and 3.708s. For ease of observation, the overall change amplitude at the peak moments of 3.0536s and 3.448s was amplified by 12 times.

From Figure 5 (a), it can be seen that at 2.852 seconds, the overall structure of the liquid rocket is basically in a vertical state, that is, perpendicular to the xy plane; From Figure 5 (b), it can be seen that at 3.0536 seconds, the top of the liquid rocket is the minimum displacement point, with a displacement of approximately 0.2157 meters, swinging in the negative x-axis direction; According to Figure 5 (c), it can be seen that at 3.448s, the top of the liquid rocket is the position with the maximum displacement, which is about 0.1533m and swings in the positive direction towards the x-

axis; As shown in Figure 5 (d), at 3.708 seconds, the overall structure of the liquid rocket returned to a vertical state. From Figures 5 (a) to (d), it can be seen that the displacement value increases with the increase of height.

The total displacement trend of the liquid rocket during one oscillation cycle after refueling under the influence of EI waves is the same as before refueling, with the maximum displacement occurring at the top and the minimum displacement at the bottom. According to the characteristics of the cycle, the same trend can be observed throughout the entire time history. But after adding propellant, the rocket's swing significantly increased, the cycle also became longer, and the swing was not stable within 5 seconds. This indicates that after refueling, under the action of EI waves, the inertial oscillation of the propellant is strengthened, and there is a possibility of divergence, ultimately causing the liquid rocket to tip over. Therefore, in order to prevent the danger of missiles under strong seismic action, the constraints of the clamps on the launch tower on the rocket should not be lifted too early.

4.4. Equivalent stress of rocket after filling under EI wave

When analyzing the effect forces such as the filling condition, the equivalent stress nephogram at the initial, trough, peak and end of the stable period is also selected for analysis, as shown in Figure 6. Equivalent stress nephogram corresponding to 2.852s, 3.0536s, 3.448s and 3.708s. For the convenience of observation, the overall change amplitude at the peak time of 3.0536s and 3.448s was amplified by 12 times.

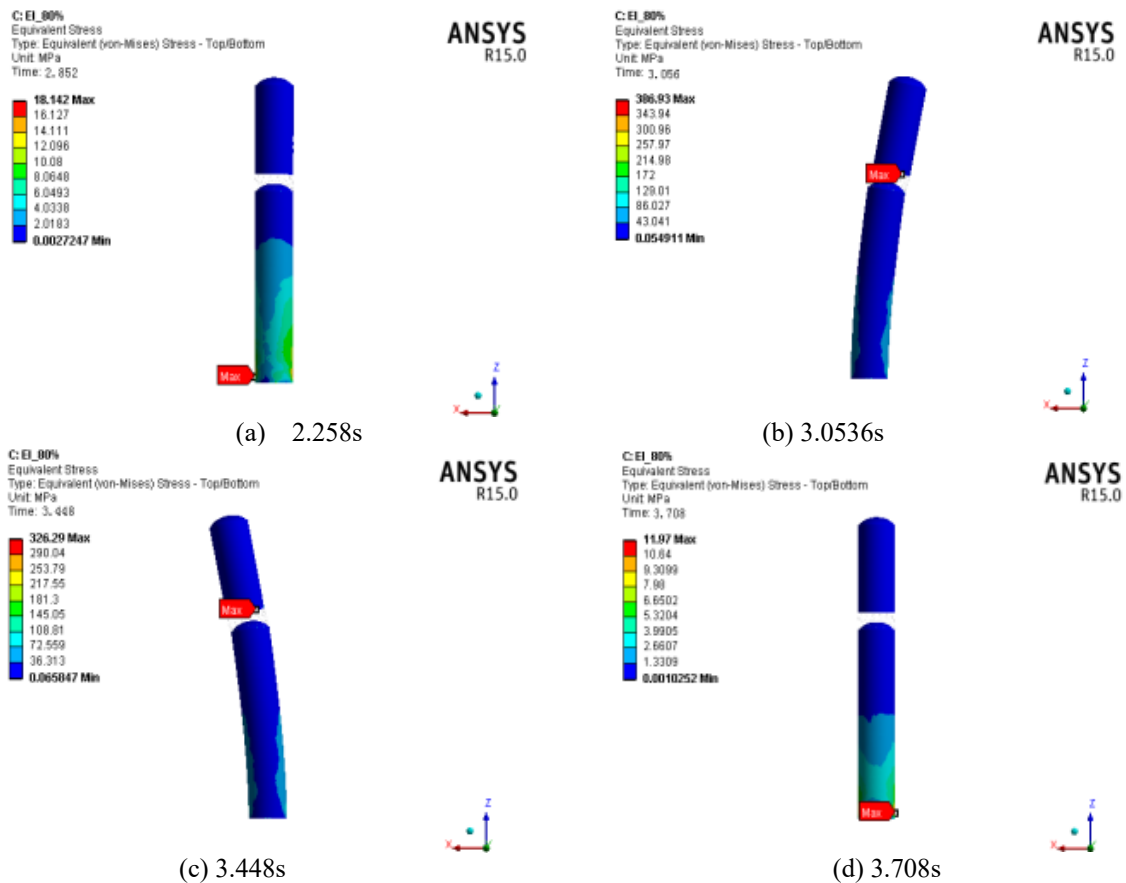


Figure 6. Equivalent Stress Nephogram of Rocket Under Earthquake Wave EI After Fueling

It can be seen from Figure 6 that the maximum stress of the liquid rocket after filling also appears near the fixed support constraint. When the liquid rocket swings to the maximum displacement, the maximum stress value is about 386MPa. When the liquid rocket swings back to the initial upright state, the maximum stress value is about 12~17MPa. Therefore, it can be seen that the maximum stress in the whole swing process occurs at the moment of maximum swing amplitude.

Further analysis of the stress data shows that the maximum stress value of the liquid rocket after filling under the action of EI wave is about 390MPa, which is close to the yield limit of the material itself. Although there is no plastic deformation, when the safety factor is 1.5, the safety reserve factor of the structure is 0.6, indicating that the structure of the liquid rocket after filling has suffered strength failure under the action of EI wave, which should be strengthened in the design.

It can also be seen from the analysis that the stress of the liquid rocket after filling in the area near the second stage tail section and interstage rod section is also large under the action of the whole EI wave, and the interstage rod section is subject to large tensile and compressive stress, which reaches 230MPa, and there is a possibility of instability, which should be paid enough attention to.

5. Conclusion

The analysis results show that under the action of EI seismic wave, the liquid rocket oscillates along the direction of seismic wave before and after filling. With the increase of rocket height, the swing amplitude increases, the maximum swing amplitude appears at the top of the rocket, and the maximum equivalent stress appears near the support part of the rocket tail. But before filling, the swing amplitude and equivalent stress are small, which will not affect the stability and structural safety of the rocket. After filling, the swing amplitude and equivalent stress increase significantly, the rocket may topple, the support part of the rocket tail may have strength failure, and the stress of the interstage rod section is also large, which may have instability failure, which should also be paid enough attention to.

References

- [1] Zhou Xiaofu, Kang Yanbo, Zhang Rongqiang et al. An overview of the development of modern architecture and seismic technology and the development trend of modern buildings[J]. *Building Science*, 2021, 37(1):114-120.
- [2] Zhang Rulin, Cheng Xudong, Guan Youhai. A review of the current status and development of seismic research on large storage tanks[J]. *Sichuan Research on Building Science*, 2015, 41(1): 205-209.
- [3] Fang Hao, Wu Hao, Wang Duguo. A review of research on seismic safety of liquid storage tanks[J]. *Earthquake Defense Technology*, 2012, 7(2):144-151.
- [4] Zhang Rulin, Cheng Xudong, Wang Huaifeng. Analysis of the effect of vertical seismic action on the seismic response of liquid storage tanks[J]. *Journal of Earthquake Engineering*, 2017, 39(4):592-599.
- [5] Sun Dan, Mao Yuming, Di Wenbin et al. Current status and outlook of the development of structural dynamics modeling technology for launch vehicles[J]. *China Aerospace*, 2022, Issue 9: 26-30.
- [6] Wang Jianmin, Wu Yanhong, Zhang Zhong. Three-dimensional modeling technology for full-arrow dynamic characteristics of launch vehicles[J]. *Science China*, 2014, 44(1):50-61.
- [7] Zhou Sida, Liu Li. A review of methods for analyzing fluid-structure coupling in launch vehicle storage tanks[J]. *Strength and Environment*, 2010, 37(3):52-63.
- [8] Zhu Changfan, Tang Guoan, Zhang Meiyuan. Comparison algorithm for liquid-solid coupling analysis of rockets considering propellant wobble[J]. *Journal of Dynamics and Control*, 2014, 12(3):239-242.
- [9] Liu Caizhi, Tang Guojin. Seismic response analysis and damping design of a certain launch vehicle[J]. *Journal of National University of Defense Technology*, 2014, 36(4):27-32.
- [10] Pan Zhongwen, Xing Yufeng, Zhu Liwen. Liquid propellant simulation technology in launch vehicle dynamics modeling[J]. *Science China*, 2010, 40(8):920-928.